NRL Report 5749

SMALL-SIGNAL ANALYSIS OF MONOTRONS USING A CIRCULAR CYLINDRICAL TM $_{\ell mn}$ RESONATOR

H. D. Arnett

Electron Tubes Branch
Electronics Division

March 16, 1962

U. S. NAVAL RESEARCH LABORATORY
Washington, D.C.

CONTENTS

ABSTRACT

This report presents a theoretical treatment of the small-signal aspects of the generation of microwave power by passing an electron beam axially through a circular cylindrical cavity, where the beam interacts with the axial component of the electric field of the transverse magnetic modes of the cavity. The most favorable conditions for oscillation occur when the transit time is such that an unmodulated electron requires approximately $q + (1/4) \cos n\pi$ periods of the oscillation in traveling through the cavity. The small-signal electronic efficiencies are computed and plotted, and under the assumption that the power dissipated within the cavity can be attributed solely to skin-effect losses in the cavity walls, the unloaded starting currents are computed. It is shown that, from the standpoint of minimizing the starting current, the best mode to employ is the TM_{011} mode. Further, the starting current for the TM_{011} mode is minimized when the ratio of cavity length to cavity diameter is 1.544.

PROBLEM STATUS

This is an interim report; work on the problem is continuing.

AUTHORIZATION

NRL Problem R08-03
Projects RR 008-03-46-5650 and
SR 008-03-02, Task 9491
BuShips No. S-1956

Manuscript submitted January 16, 1962.

SMALL-SIGNAL ANALYSIS OF MONOTRONS USING A CIRCULAR CYLINDRICAL $TM_{\ell mn}$ RESONATOR

INTRODUCTION

Microwave power, generated by electron tubes operating on the velocity-modulation principle, results from the interaction of an electron beam with high-frequency electric fields in such a way that some of the steady-state, or dc, beam power is converted into high-frequency electromagnetic power. In the two-cavity klystron, for example, this transformation takes place in three well-defined steps. First, the electron velocity is periodically varied by the high-frequency electric field at the buncher gap. Second, those electrons that have gained velocity overtake electrons that have lost velocity, and the electron beam becomes bunched in the drift region between the buncher and catcher gaps. Third, as these bunches traverse the catcher gap, high-frequency electromagnetic power is extracted from the beam.

For more than two decades it has been recognized that an electron beam making a single passage through a single-gap resonant cavity (1,2) is capable of exciting oscillations in the cavity. This is so, even though the beam is unmodulated as it enters the resonator. In this type of electron device, usually called a monotron, the processes of velocity variation, bunching, and catching take place simultaneously rather than sequentially, as is the case for the conventional klystron.

It is the purpose of this report to develop those features of the monotron that can be determined by considering only the presence of infinitesimal field strengths within the monotron cavity. To do this, it is necessary to consider two quite distinct aspects of the overall problem. The first is associated with the electron beam as it exists in the field configuration of the monotron cavity. This entails solving the equation of motion for electrons moving through the cavity, and it is the transcendental nature of this equation that makes it difficult to solve except for the case of small fields. The second aspect of the problem is associated with the resonant cavity, the output coupler, and the load considered purely as passive circuit elements. This involves only rather obvious extensions of microwave circuit theory. From the first of these considerations it is possible to establish the transit-time conditions that are favorable for the onset of oscillations. By combining the results of the two aspects of the problem, it is possible to predict the minimum beam current, called the starting current, necessary for maintaining the infinitesimal fields.

In the analysis of the properties of the monotron oscillator, rationalized mks units will be used throughout. The principal assumptions are: (a) the electron beam interacts only with the longitudinal component of electric field, (b) space-charge effects are negligible, (c) the electrons, as they enter the cavity, are uniformly distributed along the axis and constitute a single-velocity, filamentary beam, (d) power dissipated in the cavity can all be attributed to skin-effect losses in the cavity walls, and (e) relativistic effects are negligible. Of these assumptions, the one most easily eliminated is the one requiring a filamentary beam. The results can easily be extended to apply to a broad beam by considering the broad beam as being made up of a bundle of filamentary beams.

This report extends the results of an earlier NRL Report (3); also, two minor errors, which do not materially affect the results, have been eliminated.

PHYSICAL MODEL AND MATHEMATICAL PLAN

Consider an electron that is injected at time $t = 0$ with a velocity v_0 and moving in the axial direction through a right circular cylindrical cavity of length L and radius a. The cylindrical coordinates used are as shown in Fig. 1. The interior of the cavity is vacuum, and the surrounding walls are made of a metallic conductor. If the cavity resonator is oscillating in a transverse magnetic mode, the components of electric field and magnetic intensity along the coordinate directions are as shown (4) in Table 1. In Table 1, the time-dependent factor has been omitted. However, the electric field is in time quadrature with the magnetic intensity.

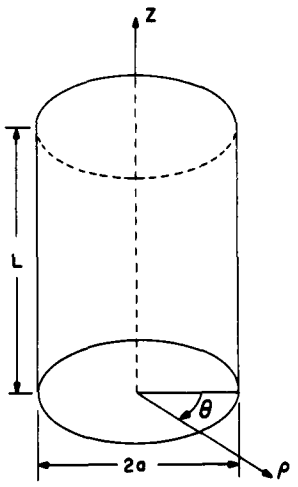

Fig. 1 - Circular cylindrical cavity. Indicated in the drawing are the dimensions of the cylinder (L and a) and the coordinate system employed (ρ, θ, z).

An electron traversing the cavity at a distance b from the axis sees an axial component of electric field given by

$$E_1 J_\ell (k_1 b) \cos \ell\theta \cos \frac{n\pi z}{L} \sin(\omega t + \phi) = \hat{E} \cos \frac{n\pi z}{L} \sin(\omega t + \phi)$$

where ω is the resonant radian frequency for the mode considered, and ϕ is the phase of the electric field as the electron enters the cavity (at $z = 0$). In accordance with assumption (a), this is the only field that affects the electron's motion (a state of affairs that can be achieved, for example, by applying a strong dc magnetic field in the z-direction), and so the equation of motion for the electron while it is in the cavity is

$$\frac{d^2 z}{dt^2} = - \frac{e}{m_e} \hat{E} \cos \frac{n\pi z}{L} \sin(\omega t + \phi), \qquad (1)$$

where e is the magnitude of the electron's charge, and m_e is its mass.

Table 1
Components of Electric Field and Magnetic Intensity Along the Coordinate Directions of a Circular Cylindrical Cavity Oscillating in a Transverse Magnetic (TM) Mode

$$E_\rho = \frac{k_3}{k_1} E_1 J'_\ell (k_1 \rho) \cos \ell\theta \sin k_3 z$$

$$E_\theta = \ell \frac{k_3}{k_1^2 \rho} E_1 J_\ell (k_1 \rho) \sin \ell\theta \sin k_3 z$$

$$E_z = E_1 J_\ell (k_1 \rho) \cos \ell\theta \cos k_3 z$$

$$H_\rho = -\ell \sqrt{\frac{\epsilon_0}{\mu_0}} \frac{k}{k_1^2 \rho} E_1 J_\ell (k_1 \rho) \sin \ell\theta \cos k_3 z$$

$$H_\theta = -\sqrt{\frac{\epsilon_0}{\mu_0}} \frac{k}{k_1} E_1 J'_\ell (k_1 \rho) \cos \ell\theta \cos k_3 z$$

$$H_z = 0$$

where

$k_1 a = r_{\ell m}$ ($r_{\ell m}$ = mth zero of $J_\ell (x)$)

$$k_3 = \frac{n\pi}{L}$$

$$k = \frac{2\pi}{\lambda} \text{ and } k^2 = k_1^2 + k_3^2$$

and

ϵ_0 = permittivity of free space

μ_0 = permeability of free space

λ = free-space wavelength

ℓ, m, n = integral indices identifying the modes

The acceleration produced by the axial electric field causes the electron to change its velocity so that the electron exits from the cavity (at $z = L$) with a velocity v_1. Thus, an increment of energy

$$\Delta W = \frac{1}{2} m_e (v_0^2 - v_1^2) \tag{2}$$

is transferred from kinetic energy of the electron to electromagnetic field energy of the cavity. The conversion efficiency is given by

$$\eta_e = \frac{\Delta W}{W} = 1 - \frac{v_1^2}{v_0^2}, \tag{3}$$

where

$$W = \frac{1}{2} m_e v_0^2 \tag{4}$$

is the amount of kinetic energy possessed by the electron as it enters the cavity. With all other parameters of the system held constant, the conversion efficiency applicable to an electron stream satisfying assumption (c) is given by Eq. (3) averaged over all initial phases, i.e., by

$$\langle \eta_e \rangle = \frac{1}{2\pi} \int_0^{2\pi} \eta_e \, d\phi. \tag{5}$$

Depending on the value of the dc transit angle, $\langle \eta_e \rangle$ may be either positive or negative. One of the requirements for oscillation to be maintained is that $\langle \eta_e \rangle$ must be positive.

If the stream of electrons constitutes a beam current of value I_0, and if V_0 is the voltage required to give the electrons the velocity v_0, the rate at which electron kinetic energy is converted into electromagnetic field energy is

$$\frac{dW}{dt} = \langle \eta_e \rangle I_0 V_0. \tag{6}$$

The electromagnetic power generated in accordance with Eq. (6) is dissipated partly in the cavity walls and partly in the load that is coupled to the cavity. The rate at which electromagnetic energy flows into these two sinks can be expressed, using well-known microwave cavity theory, by

$$\frac{dW}{dt} = \frac{1}{2} G \left(\hat{E}L\right)^2, \tag{7}$$

where the conductance G is a function only of the cavity geometry, mode indices, conductivity of the metallic walls, and the load coupling.

Conservation of energy requires, for steady-state oscillations, that the electric field take on a value such that the rate of electronic energy conversion be equal to the rate of energy dissipation, or

$$\langle \eta_e \rangle I_0 V_0 = \frac{1}{2} G \left(\hat{E}L\right)^2. \tag{8}$$

The determination of $\langle \eta_e \rangle$ requires the integrations of Eq. (1), subject to the boundary conditions

$$\frac{dz}{dt} = v_o \quad \text{and} \quad z = 0 \quad \text{when} \quad t = 0.$$

The form of the equation and the nature of the boundary conditions make it impossible to find v_1 in a closed form. In the next section, an iterative procedure is employed to obtain a value of v_1, sufficient to calculate $\lim_{\hat{E} \to 0} \langle \eta_e \rangle / \hat{E}^2$. This is then sufficient to calculate the minimum current required to maintain oscillations and leads to an expression for the starting current, given by

$$I_S = \frac{GL^2}{2V_0} \lim_{\hat{E} \to 0} \frac{\hat{E}^2}{\langle \eta_e \rangle}. \tag{9}$$

In the next section, the electron interaction problem will be dealt with. In succeeding sections of the report, microwave cavity theory will be developed to compute the value of the cavity conductance G and to determine to what extent it can be optimized.

SMALL-SIGNAL ELECTRONIC EFFICIENCY

Before attempting the integration of Eq. (1), dimensionless variables and parameters will be used to write Eq. (1) in the form

$$\ddot{\zeta} = -\alpha \cos\left(\frac{n\pi\zeta}{\zeta_0}\right) \sin(\tau + \phi), \tag{10}$$

where the following definitions apply:

$$\tau = \omega t, \tag{11}$$

$$\zeta = \frac{\omega z}{v_0}, \tag{12}$$

$$\zeta_0 = \frac{\omega L}{v_0}, \tag{13}$$

$$\alpha = \frac{e\hat{E}}{m_e \omega v_0} = \frac{\hat{E}L}{2V_0 \zeta_0}. \tag{14}$$

The Newtonian dot notation designates differentiation with respect to τ. The parameter ζ_0 is the dc transit angle, in radians, of an electron traversing the length of the cavity. The parameter α is a measure of the amplitude of the oscillating field and will be called the modulation parameter. The initial conditions which must be imposed on the solutions of Eq. (10) are

$$\dot{\zeta} = 1 \quad \text{and} \quad \zeta = 0 \quad \text{when} \quad \tau = 0. \tag{15}$$

For the special case of $n = 0$, Eq. (10) can be integrated to give

$$\dot{\zeta} = 1 + \alpha \left[\cos(\tau + \phi) - \cos\phi\right] \tag{16}$$

and

$$\zeta = \tau + \alpha\,[\sin(\tau + \phi) - \tau\cos\phi - \sin\phi]. \tag{17}$$

To find the electronic efficiency, it is necessary to know $\dot{\zeta}$ as a function of ζ rather than of τ. Specifically, it is necessary to know the normalized electron velocity when the electron, characterized by initial phase ϕ, departs from the cavity. If this exit velocity is denoted $\dot{\zeta}_1$ and the corresponding time τ_1, since the normalized exit position is ζ_0, it is necessary to solve the equation

$$\zeta_0 = \tau_1 + \alpha\,[\sin(\tau_1 + \phi) - \tau_1\cos\phi - \sin\phi] \tag{18}$$

for τ_1 and substitue this value into Eq. (16) to give $\dot{\zeta}_1$. Because of the transcendental nature of Eq. (18), this solution cannot be found in closed form. The terms in Eq. (18) involving τ_1 can be expanded into a Taylor series about $\tau_1 = \zeta_0$ to give the exit time to any degree of accuracy. This is essentially the procedure employed by Müller and Rostas (1) in developing a large-signal theory for the case $n = 0$.

For the general case, $n \neq 0$, direct integration of Eq. (10) is not possible. Hence a procedure of series approximation is adopted one step earlier. The form of Eq. (17) suggests writing the solution of Eq. (10) in the form

$$\zeta = \tau + \alpha f_1(\tau,\phi) + \alpha^2 f_2(\tau,\phi) + \cdots + \alpha^n f_n(\tau,\phi) + \cdots. \tag{19}$$

When Eq. (19) is used to express both sides of Eq. (10) as Maclaurin series in α, the following set of differential equations emerges:

$$\ddot{f}_1(\tau,\phi) = -\cos\left(\frac{n\pi\tau}{\zeta_0}\right)\sin(\tau + \phi), \tag{20}$$

$$\ddot{f}_2(\tau,\phi) = \frac{n\pi}{\zeta_0} f_1(\tau,\phi)\sin\left(\frac{n\pi\tau}{\zeta_0}\right)\sin(\tau + \phi), \tag{21}$$

$$\ddot{f}_3(\tau,\phi) = \frac{n\pi}{\zeta_0}\left[\frac{n\pi}{\zeta_0} f_1^2(\tau,\phi)\cos\left(\frac{n\pi\tau}{\zeta_0}\right) + f_2(\tau,\phi)\sin\left(\frac{n\pi\tau}{\zeta_0}\right)\right]\sin(\tau + \phi), \tag{22}$$

etc., when coefficients of like powers of α are equated.

Because of the increasing complexity of Eqs. (20) to (22), the temptation to develop, by this method, a large-signal theory of the monotron for $n \neq 0$ is one that is easy to resist. Therefore, the solution will be carried only far enough to give the electron exit velocity to the lowest significant order in α (i.e., to terms in α^2). To do this, it is necessary to calculate $\dot{f}_1(\tau,\phi)$, $f_1(\tau,\phi)$, and $\dot{f}_2(\tau,\phi)$ by

$$\dot{f}_1(\tau,\phi) = -\int_0^\tau \cos\left(\frac{n\pi\tau'}{\zeta_0}\right)\sin(\tau' + \phi)\,d\tau', \tag{23}$$

$$f_1(\tau,\phi) = \int_0^\tau \dot{f}_1(\tau',\phi)\,d\tau', \tag{24}$$

$$\dot{f}_2(\tau,\phi) = \frac{n\pi}{\zeta_0}\int_0^{\tau} f_1(\tau',\phi)\sin\left(\frac{n\pi\tau'}{\zeta_0}\right)\sin(\tau'+\phi)\,d\tau'. \tag{25}$$

The integration of Eqs. (23) to (25) is straightforward but tedious.

Again it is necessary to express the electron exit velocity

$$\dot{\zeta}_1 = 1 + \alpha\dot{f}_1(\tau_1,\phi) + \alpha^2\dot{f}_2(\tau_1,\phi) + \cdots \tag{26}$$

in terms of ζ_0. This is done by using

$$\zeta_0 = \tau_1 + \alpha f_1(\tau_1,\phi) + \cdots. \tag{27}$$

An expression for $\dot{\zeta}_1$, accurate to the order of α^2, is obtained by using $\tau_1 = \zeta_0$ in the third term on the right of Eq. (26) and $\tau_1 = \zeta_0 - \alpha f_1(\zeta_0,\phi)$ in the second term, and then expanding the second term. The resulting expression for $\dot{\zeta}_0$, correct to the order of α^2, is

$$\dot{\zeta}_1 = 1 + \alpha\dot{f}_1(\zeta_0,\phi) + \alpha^2\left[\dot{f}_2(\zeta_0,\phi) - f_1(\zeta_0,\phi)\ddot{f}_1(\zeta_0,\phi)\right]. \tag{28}$$

The fraction of its energy that an electron, with initial phase ϕ, gives to the oscillating field is given by

$$\eta_e = 1 - \dot{\zeta}_1^2. \tag{29}$$

The small-signal electronic efficiency (designated η_{eS}) is therefore given by

$$\eta_{eS} = -2\alpha\dot{f}_1(\zeta_0,\phi) + \alpha^2\left[2f_1(\zeta_0,\phi)\ddot{f}_1(\zeta_0,\phi) - \dot{f}_1^2(\zeta_0,\phi) - 2\dot{f}_2(\zeta_0,\phi)\right]. \tag{30}$$

The average small-signal electronic efficiency for a stream of electrons, distributed uniformly in initial phase, is given by

$$\langle\eta_{eS}\rangle = \frac{1}{2\pi}\int_0^{2\pi}\eta_{eS}\,d\phi, \tag{31}$$

and since the integral of the coefficient of α in Eq. (30) vanishes,

$$\langle\eta_{eS}\rangle = \frac{\alpha^2}{2\pi}\int_0^{2\pi}\left[2f_1(\zeta_0,\phi)\ddot{f}_1(\zeta_0,\phi) - f_1^2(\zeta_0,\phi) - 2\dot{f}_2(\zeta_0,\phi)\right]d\phi. \tag{32}$$

The end result of this procedure is

$$\frac{\langle\eta_{eS}\rangle}{\alpha^2} = \frac{\left(1-\frac{n^2\pi^2}{\zeta_0^2}\right)\zeta_0\sin\zeta_0\cos n\pi + 2\left(1+\frac{n^2\pi^2}{\zeta_0^2}\right)(\cos\zeta_0\cos n\pi - 1)}{\left(1-\frac{n^2\pi^2}{\zeta_0^2}\right)^3}. \tag{33}$$

Graphs of the ratio of small-signal electronic efficiency to the square of the modulation parameter as a function of dc transit angle are shown in Fig. 2 for $n = 0, 1, 2$, and 3. Sustained oscillations are possible for the values of transit angle that give positive electronic efficiency.

For large values of ζ_0, the first term in the numerator of Eq. (33) predominates. Hence, for large values of ζ_0 the maximum value of $\langle \eta_{eS} \rangle / a^2$ occurs when $\sin \zeta_0 \cos n\pi = 1$, or

$$(\zeta_0)_{optimum} = 2\pi \left(q + \frac{\cos n\pi}{4} \right), \tag{34}$$

where q is an integer. A table of optimum values of transit angle and corresponding values of $\langle \eta_{eS} \rangle / a^2$ is given in Table 2 for $n = 0, 1, 2$, and 3. For larger values of q than those tabulated, an error of less than 0.1 percent will result if Eq. (34) is substituted into Eq. (33).

MONOTRON STARTING CURRENT

Turning now to the circuit aspects of the problem, use is made of the relations given in Table 1 and Eqs. (7) and (9). In computing the power dissipated inside the cavity, it is assumed that the interior cavity surface has a uniform surface resistivity (R_s) and that this surface resistivity is given by the standard skin-effect formulas. Also Eq. (9) can be written, using definitions introduced in the previous section, as

$$I_S = \frac{m_e c^2}{e} \left(\frac{L}{a} \right)^2 r_m^2 \left(\frac{k}{k_1} \right)^2 G \lim_{a \to 0} \frac{a^2}{\langle \eta_e \rangle}, \tag{35}$$

where c is the velocity of light in vacuum.

It is necessary to distinguish between two starting currents, depending on whether G is a measure of the power dissipated inside the cavity or whether it measures the power dissipated in the load as well as in the cavity. In the first case the unloaded starting current (I_{SU}) is obtained, and in the second case the loaded starting current (I_{SL}) is obtained. These are related by the expression

$$I_{SL} = I_{SU} \frac{Q_U}{Q_L}, \tag{36}$$

where Q_U is the unloaded quality factor and Q_L is the loaded quality factor. Since the unloaded starting current depends only on the properties of the cavity, while the loaded starting current also depends upon the degree of coupling to the load, only the unloaded starting current will be calculated here. It should be remembered, however, that in an experimental situation it is the loaded starting current that must be exceeded before oscillations are attained.

The power dissipated in the cavity walls (P_{cav}) is given by

$$P_{cav} = \frac{R_s}{2} \int_s |H_t|^2 \, dS, \tag{37}$$

where R_s is the surface resistivity, and H_t is the tangential component of magnetic field intensity at the cavity walls. The surface integral is to be evaluated over the entire

(a) the $TM_{\ell_{m0}}$ modes

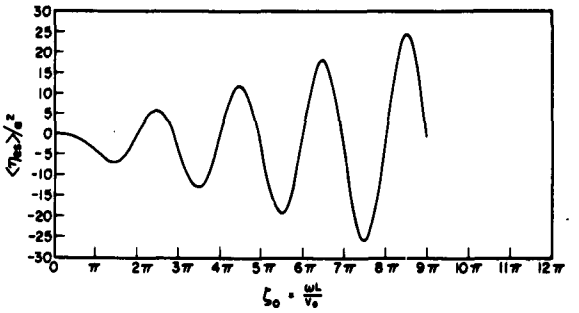

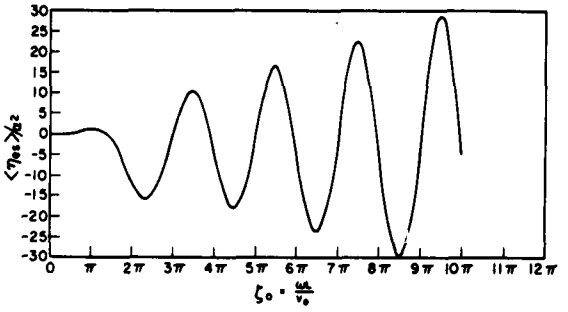

(b) the $TM_{\ell_{m1}}$ modes

(c) the $TM_{\ell_{m2}}$ modes

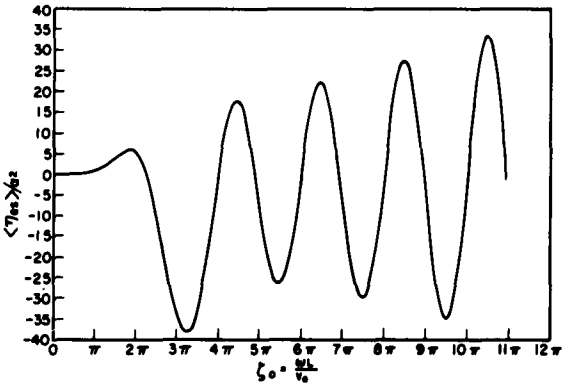

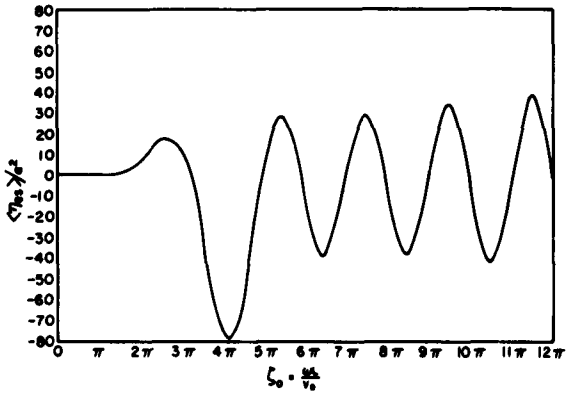

(d) the $TM_{\ell_{m3}}$ modes

Fig. 2 - Plot of the small-signal efficiency parameter $\langle \eta_{es} \rangle / a^2$ as a function of dc transit angle

Table 2
Optimum Values of DC Transit Angle (ζ_0) and Small-Signal Efficiency Parameter ($\langle\eta_{eS}\rangle/\alpha^2$) for n = 0, 1, 2, and 3

n	$(\zeta_0)_{opt}/\pi$	q	$\lim_{\alpha\to 0} \frac{\langle\eta_e\rangle}{\alpha^2}\Big\|_{max} = \frac{\langle\eta_{eS}\rangle}{\alpha^2}\Big\|_{max}$
0	2.46	1	5.92
0	4.46	2	12.17
0	6.48	3	18.44
0	8.49	4	24.72
1	3.45	2	10.38
1	5.48	3	16.24
1	7.48	4	22.30
1	9.49	5	28.48
2	4.44	2	17.71
2	6.47	3	22.06
2	8.48	4	27.47
2	10.49	5	33.23
3	5.43	3	28.40
3	7.47	4	29.65
3	9.48	5	33.88
3	11.49	6	39.00

interior surface of the cavity. From the values of magnetic field intensity given in Table 1,

$$P_{cav} = R_s \frac{\epsilon_0}{\mu_0}\left(\frac{k}{k_1}\right)^2 E_1^2 \left\{ \frac{a J_\ell'^2 (r\ell_m)}{2} \int_0^L \int_0^{2\pi} \cos^2 k_3 z \cos^2 \ell\theta \, d\theta dz \right.$$

$$\left. + \int_0^a \int_0^{4\pi} \rho \left[J_\ell'^2 (k_1 \rho) \cos^2 \ell\theta + \frac{\ell^2}{k_1^2 \rho^2} J_\ell^2 (k_1 \rho) \sin^2 \ell\theta \right] d\theta d\rho \right\}. \quad (38)$$

The evaluation of the first double integral of Eq. (38) is elementary. The second one is simplified by the Bessel-function identity

$$J_\ell' (k_1 \rho) = -\frac{\ell}{k_1 \rho} J_\ell (k_1 \rho) + J_{\ell-1} (k_1 \rho)$$

and by using the fact that $J_\ell (k_1 a) = 0$. The result is

$$P_{cav} = \frac{\pi a^2}{2} h(\ell) R_s \frac{\epsilon_0}{\mu_0}\left(\frac{k}{k_1}\right)^2 E_1^2 J_\ell'^2 (r\ell_m)\left[\frac{h(n) L}{2a} + 1\right], \quad (39)$$

where

$$h(\ell) = \begin{cases} 2, & \text{when } \ell = 0 \\ 1, & \text{when } \ell \neq 0 \end{cases} \tag{40}$$

A similar relation holds for $h(n)$. From Eq. (39) it follows that

$$G_{cav} = \pi h(\ell) \left(\frac{a}{L}\frac{k}{k_1}\right)^2 \frac{\epsilon_0}{\mu_0} R_s \left[1 + \frac{h(n)\,L}{2a}\right] \frac{J_\ell'^2 (r_{\ell m})}{\cos^2 \ell\theta\, J_\ell^2 \left(r_{\ell m}\frac{b}{a}\right)}. \tag{41}$$

Expressing the surface resistivity R_s in terms of the skin depth ($R_s = 1/\sigma\delta$), Eq. (41) becomes

$$G_{cav}\frac{\lambda}{\delta} = \pi^2 h(\ell) \left(\frac{a}{L}\frac{k}{k_1}\right)^2 \sqrt{\frac{\epsilon_0}{\mu_0}} \left[1 + \frac{h(n)\,L}{2a}\right] \frac{J_\ell'^2 (r_{\ell m})}{\cos^2 \ell\theta\, J_\ell^2 \left(r_{\ell m}\frac{b}{a}\right)}, \tag{42}$$

with

$$\delta = \sqrt{\frac{2}{\omega \mu_0 \sigma}},$$

where σ is the bulk conductivity of the cavity material. Now combining Eqs. (35) and (42)

$$I_{SU}\frac{\lambda}{\delta} = \frac{\pi^2 m_e c^2}{e} h(\ell) \sqrt{\frac{\epsilon_0}{\mu_0}} \left(\frac{k}{k_1}\right)^4 \left[1 + \frac{h(n)\,L}{2a}\right] \frac{r_{\ell m}^2 J_\ell'^2 (r_{\ell m})}{\cos^2 \ell\theta\, J_\ell^2 \left(r_{\ell m}\frac{b}{a}\right)} \lim_{a \to 0} \frac{a^2}{\langle \eta_e \rangle}. \tag{43}$$

Using the dispersion relation $k^2 = k_1^2 + k_3^2$, Eq. (43) can be written in such a way that the unloaded starting current is written explicitly as a function of the ratio of cavity length to cavity radius (or diameter) and also as a function of the ratio of cavity length to resonant wavelength. As a function of L/D, the ratio of cavity length to cavity diameter,

$$I_{SU}\frac{\lambda}{\delta} = \frac{\pi^2 m_e c^2}{e} h(\ell) \sqrt{\frac{\epsilon_0}{\mu_0}} \left[1 + \frac{n^2\pi^2}{4 r_{\ell m}^2}\left(\frac{D}{L}\right)^2\right]^2 \left[1 + h(n)\frac{L}{D}\right] \frac{r_{\ell m}^2 J_\ell'^2 (r_{\ell m})}{\cos^2 \ell\theta\, J_\ell^2 \left(r_{\ell m}\frac{b}{a}\right)} \lim_{a \to 0} \frac{a^2}{\langle \eta_e \rangle}, \tag{44}$$

and as a function of L/λ,

$$I_{SU}\frac{\lambda}{\delta} = \frac{\pi^2 m_e c^2}{e} h(\ell) \sqrt{\frac{\epsilon_0}{\mu_0}} \frac{\left\{1 + \frac{n\pi h(n)}{2 r_{\ell m}}\left[\frac{4}{n^2}\frac{L^2}{\lambda^2} - 1\right]^{1/2}\right\}}{\left(1 - \frac{n^2}{4}\frac{\lambda^2}{L^2}\right)^2} \frac{r_{\ell m}^2 J_\ell'^2 (r_{\ell m})}{\cos^2 \ell\theta\, J_\ell^2 \left(r_{\ell m}\frac{b}{a}\right)} \lim_{a \to 0} \frac{a^2}{\langle \eta_e \rangle}. \tag{45}$$

Graphs of $I_{SU}\lambda/\delta$ as a function of L/D are shown in Fig. 3 and as a function of L/λ in Fig. 4 for some of the TM_{01n} cavity modes of oscillation. In all of these graphs, optimum values of $\lim_{a \to 0} a^2/\langle \eta_e \rangle$ are used and $b = 0$. In spite of the gain of the factor 2 obtained in

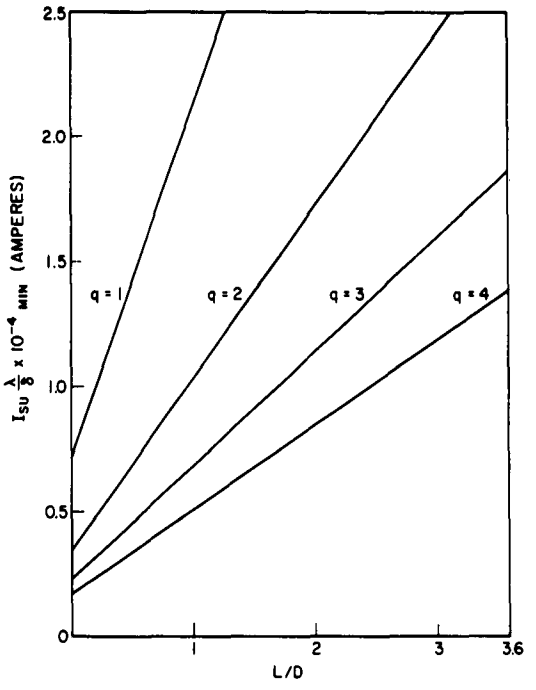

(a) the TM_{010} modes

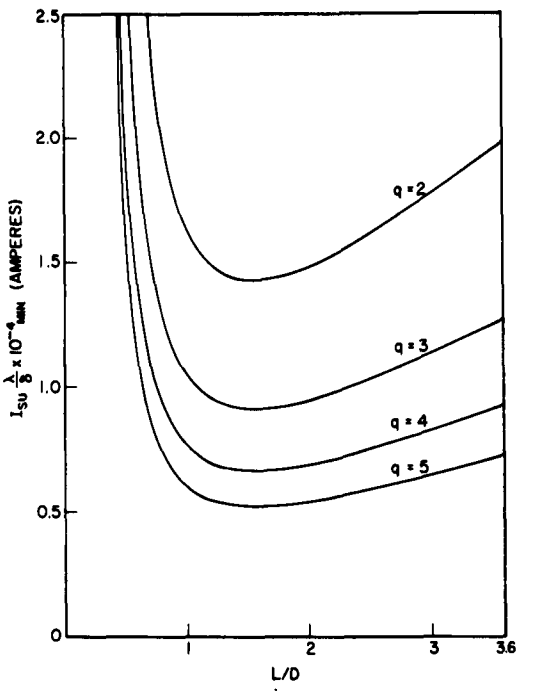

(b) the TM_{011} modes

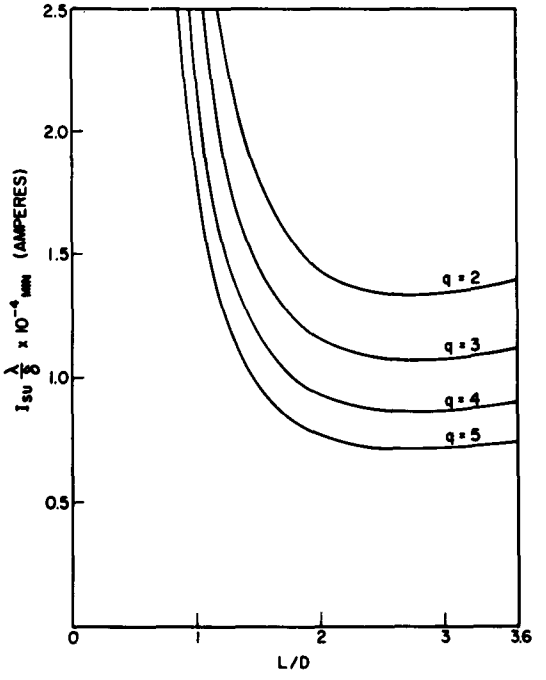

(c) the TM_{012} modes

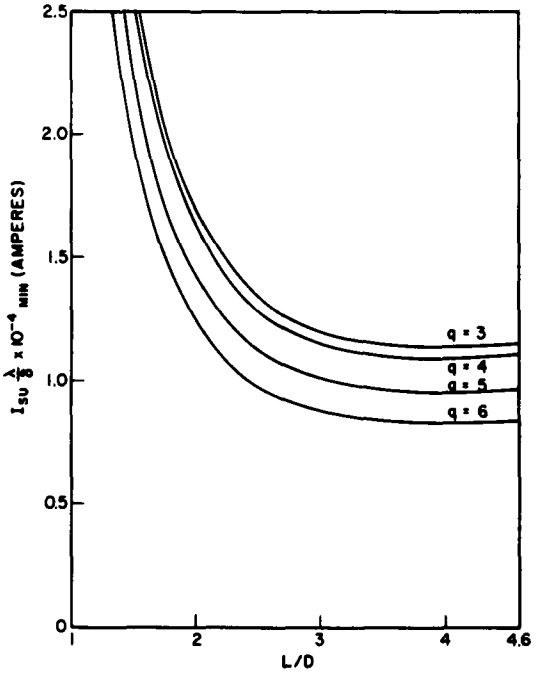

(d) the TM_{013} modes

Fig. 3 - Plot of the unloaded starting currents as a function of L/D

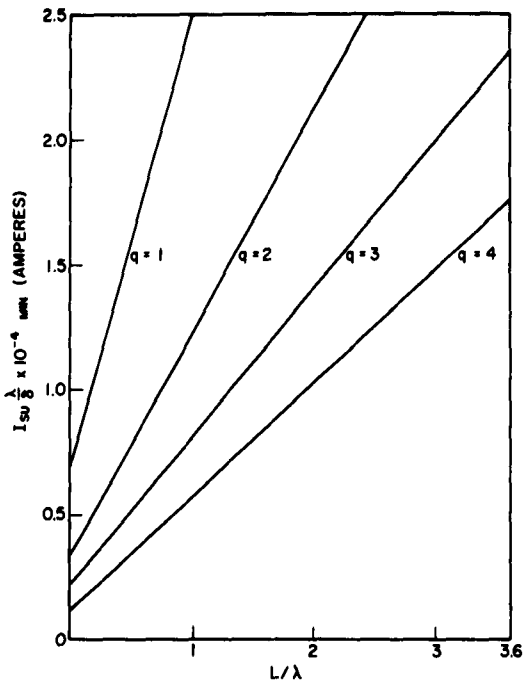

(a) the TM_{010} modes

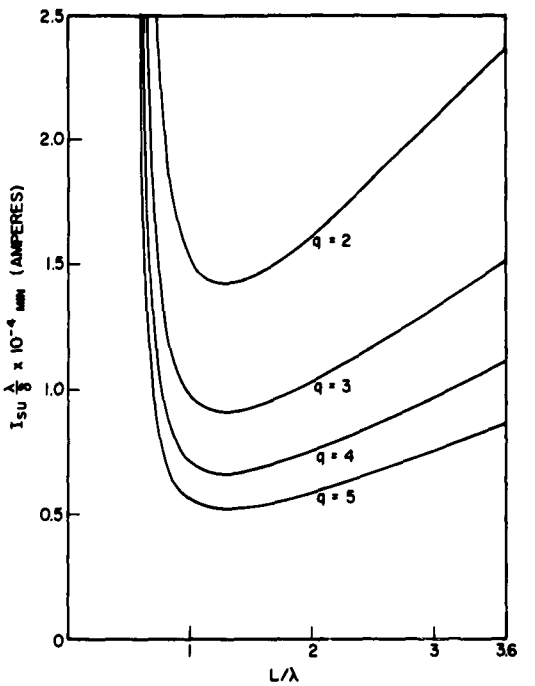

(b) the TM_{011} modes

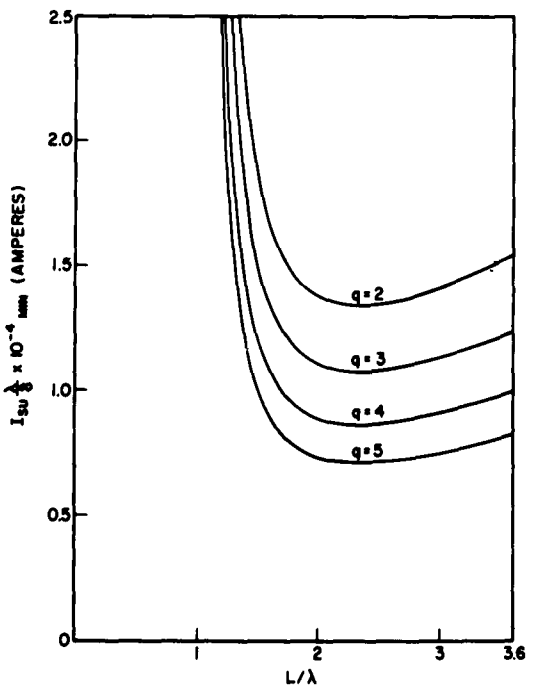

(c) the TM_{012} modes

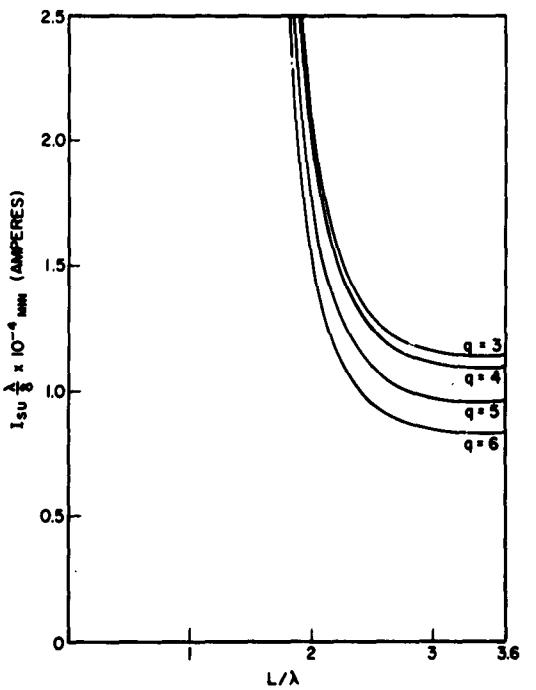

(d) the TM_{013} modes

Fig. 4 - Plot of the unloaded starting currents as a function of L/λ

the factor $h(\ell)$ when $\ell \neq 0$, the corresponding values of $r_{\ell m}$ are such that the starting current is increased under the most favorable conditions. The only advantage that could be derived from employing a cavity oscillation mode with $\ell \neq 0$ seems to be that a larger cavity size would result with, in some cases, not a greatly larger unloaded starting current. This might be an advantage from the fabrication standpoint at very short wavelengths. The use of higher order radial modes $(m > 1)$ also leads to larger cavity sizes, but with a much increased starting current. It appears, therefore, that from the standpoint of starting current alone only the TM_{010} and TM_{011} cavity modes need be considered.

A choice between the TM_{010} and TM_{011} cavity modes can be based on a third form of Eq. (43). In this, the starting current will be expressed in terms of the beam voltage (V_0). This is accomplished by using the equations $\zeta_0 = \omega L/v_0$ and $m_e v_0^2/2 = e V_0$ to give

$$\left(\frac{L}{\lambda}\right)^2 = \frac{e V_0 \zeta_0^2}{2\pi^2 m_e c^2}. \tag{46}$$

The substitution of Eq. (46) into Eq. (45) gives

$$I_{SU}\frac{\lambda}{\delta} = \frac{\pi^2 m_e c^2}{e}\sqrt{\frac{\epsilon_0}{\mu_0}}\,h(\ell)\,\frac{\left[1 + \frac{n\pi h(n)}{2r_{\ell m}}\left(\frac{V_0}{V_c} - 1\right)^{1/2}\right]}{\left(1 - \frac{V_c}{V_0}\right)^2}\,\frac{r_{\ell m}^2 J_\ell'^2(r_{\ell m})}{\cos^2 \ell\theta\, J_\ell^2\left(r_{\ell m}\frac{b}{a}\right)}\lim_{\alpha \to 0}\frac{\alpha^2}{\eta_e}, \tag{47}$$

where

$$V_c = \frac{n^2 \pi^2 m_e c^2}{2e \zeta_0^2}. \tag{48}$$

A plot of $I_{SU}\lambda/\delta$ as a function of the beam voltage (V_0) is shown in Fig. 5. In this plot the TM_{010} and TM_{011} mode starting currents are shown superimposed. It demonstrates the fact that there are two voltage regimes. In the low-voltage regime the starting currents are lowest for the TM_{010} transit-time modes; in the high-voltage regime the starting currents are lowest for the TM_{011} transit-time modes. There seems to be no better way to get the necessary beam current than to obtain it from an electron gun using a space-charge-limited cathode whose anode is at the voltage V_0. In this case the beam current increases with the 3/2 power of the beam voltage; when this is considered, the TM_{011} cavity mode is superior. It is true that for any given transit-angle condition, yielding oscillation in the TM_{011} mode, it is possible to find some transit angle that will give oscillation in the TM_{010} mode with just as small a starting current. In general the TM_{010} transit angle will be larger than the TM_{011} transit angle. It is beyond the scope of this report to demonstrate that the conversion efficiency varies approximately inversely with the transit angle. To show this requires a large-signal analysis of the force equation, but perhaps the reader who is familiar with conventional klystron theory will recall that the elementary theory of klystrons gives this same variation. Hence there is a distinct advantage for operation in the TM_{011} cavity mode.

Examination of Fig. 3 shows that there is a length-to-diameter ratio that gives a minimum starting current. For the case $n = 0$ this minimum is an end-point minimum occurring at $L/D = 0$. This condition corresponds to zero beam voltage and thus is not

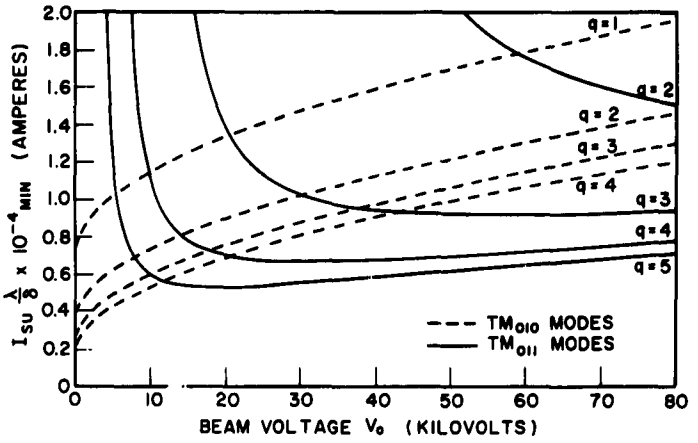

Fig. 5 - Plot of unloaded starting currents as a function of beam voltage. The TM_{010} and TM_{011} starting currents are superimposed for comparison.

significant as a design criterion. For the case $n \neq 0$ there is a definite bend-point minimum found by minimizing the expression

$$\left[1 + \frac{n^2 \pi^2}{4 r^2 \ell_m}\left(\frac{D}{L}\right)^2\right]\left(1 + \frac{L}{D}\right). \tag{49}$$

Setting the derivative of Eq. (49) with respect to L/D equal to zero gives the minimization condition

$$\left(\frac{L}{D}\right)^3 - \frac{3n^2 \pi^2}{4 r^2 \ell_m}\left(\frac{L}{D}\right) - \frac{n^2 \pi^2}{r^2 \ell_m} = 0. \tag{50}$$

This equation has one positive root and either two negative roots or two complex conjugate roots. Only the positive root has physical significance, and for the TM_{011} mode it has the approximate value

$$L/D = 1.544.$$

This ratio of L to D may or may not represent an optimum design criterion. It should be considered rather as a lower limit. By designing for a larger L/D ratio the starting current will increase, but a higher voltage will also result. The available current from an electron gun, if space charge limited, will increase more rapidly than will the starting current. It should also be noted that the L/D ratio for minimum starting current depends only on the cavity mode parameters (ℓ, m, n); it does not depend upon any of the electron beam parameters.

SUMMARY

It has been shown that for appropriate dc transit angles ζ_0, an electron beam can excite oscillations in a cylindrical cavity at any of the frequencies corresponding to the $TM_{\ell mn}$ resonant modes of the cavity. These transit angles depend only on the value of the mode index n, with the most favorable conditions for oscillation being those transit angles for which an unmodulated electron requires approximately $q + (1/4) \cos n\pi$ periods in traveling axially through the cavity (q is a positive integer). Under the assumption that the interior of the cavity is occupied by vacuum, the requirement that the electron velocity cannot exceed the velocity of light in vacuum imposes the further condition that the dc transit angle ζ_0 must equal or exceed $n\pi$.

With the assumption that the power dissipated within the cavity can all be attributed to skin-effect losses in the cavity walls, the amount of electron beam current required to maintain oscillations has been calculated. This amount of current, called the starting current, depends on all three modes indices, the transit-time parameter q, and the position of the beam with respect to the cavity axis. The minimum starting current is achieved when the TM_{011} mode is used, the beam is positioned on the cavity axis, and the ratio of the cavity length to diameter is equal to 1.544. For a cavity with fixed geometry the starting current decreases with increasing q. However, if the electron beam is obtained from a space-charge-limited cathode with an anode at cavity potential, the starting current does not fall off as rapidly as the attainable current from the electron gun. Hence, from perveance considerations and probably from efficiency considerations, it is advantageous to operate a monotron at the highest voltage for which the transit-time conditions can be satisfied. Because of its high-voltage, high-current characteristics, it is possible to achieve high power; at the same time it becomes highly desirable to attempt to recover as much as possible of the dc beam power by depressed collector techniques.

Perhaps the most striking feature of the monotron is the simplicity of the cavity. The conventional klystron cavity, due to its re-entrancy, is more difficult to construct and is smaller in physical dimensions. A monotron designed to operate at 3 centimeters, for example, with the 1.54 length-to-diameter ratio has a cylindrical cavity whose diameter is approximately one inch and whose length is approximately 1.5 inches. These advantages are of paramount importance in the millimeter wavelength range, where resonators become exceedingly small.

Since this treatment of the monotron pertains to the small-signal aspects, nothing can be concluded as to the conversion efficiency. This matter will be considered in a forthcoming report.

REFERENCES

1. Müller, J.J., and Rostas, E., "Un Générateur à Temps de Transit, Utilisant un Seul Resonateur de Volume," Helv. Phys. Acta 13:435-450 (1940)

2. Marcum, J., "Interchange of Energy Between an Electron Beam and an Oscillating Electric Field," J. Appl. Phys. 17:4-11 (Jan. 1946)

3. Arnett, H.D., and Ruhlig, A.J., "A Starting-Current Analysis of Monotrons With a Cylindrical TM_{01n} Resonator," NRL Report 4819 (Sept. 5, 1956)

4. Kinzer, J.P., and Wilson, I.G., "Some Results on Cylindrical Cavity Resonators," Bell System Tech. J. 26:410-445 (July 1947)

UNCLASSIFIED

Naval Research Laboratory. Report 5749. SMALL-SIGNAL ANALYSIS OF MONOTRONS USING A CIRCULAR CYLINDRICAL TM$_{\ell mn}$ RESONATOR, by H. D. Arnett. 16 pp. and figs., March 16, 1962.

This report presents a theoretical treatment of the small-signal aspects of the generation of microwave power by passing an electron beam axially through a circular cylindrical cavity, where the beam interacts with the axial component of the electric field of the transverse magnetic modes of the cavity. The most favorable conditions for oscillation occur when the transit time is such that an unmodulated electron requires approximately $q + (1/4) \cos n\pi$ periods of the oscillation in traveling through the cavity. The

UNCLASSIFIED (over)

1. Radio frequency power – Generation
2. Electrons – Motion – Mathematical analysis
3. Cavity resonators
- I. Monotrons
- II. Arnett, H. D.

UNCLASSIFIED

Naval Research Laboratory. Report 5749. SMALL-SIGNAL ANALYSIS OF MONOTRONS USING A CIRCULAR CYLINDRICAL TM$_{\ell mn}$ RESONATOR, by H. D. Arnett. 16 pp. and figs., March 16, 1962.

This report presents a theoretical treatment of the small-signal aspects of the generation of microwave power by passing an electron beam axially through a circular cylindrical cavity, where the beam interacts with the axial component of the electric field of the transverse magnetic modes of the cavity. The most favorable conditions for oscillation occur when the transit time is such that an unmodulated electron requires approximately $q + (1/4) \cos n\pi$ periods of the oscillation in traveling through the cavity. The

UNCLASSIFIED (over)

1. Radio frequency power – Generation
2. Electrons – Motion – Mathematical analysis
3. Cavity resonators
- I. Monotrons
- II. Arnett, H. D.

UNCLASSIFIED

Naval Research Laboratory. Report 5749. SMALL-SIGNAL ANALYSIS OF MONOTRONS USING A CIRCULAR CYLINDRICAL TM$_{\ell mn}$ RESONATOR, by H. D. Arnett. 16 pp. and figs., March 16, 1962.

This report presents a theoretical treatment of the small-signal aspects of the generation of microwave power by passing an electron beam axially through a circular cylindrical cavity, where the beam interacts with the axial component of the electric field of the transverse magnetic modes of the cavity. The most favorable conditions for oscillation occur when the transit time is such that an unmodulated electron requires approximately $q + (1/4) \cos n\pi$ periods of the oscillation in traveling through the cavity. The

UNCLASSIFIED (over)

1. Radio frequency power – Generation
2. Electrons – Motion – Mathematical analysis
3. Cavity resonators
- I. Monotrons
- II. Arnett, H. D.

UNCLASSIFIED

Naval Research Laboratory. Report 5749. SMALL-SIGNAL ANALYSIS OF MONOTRONS USING A CIRCULAR CYLINDRICAL TM$_{\ell mn}$ RESONATOR, by H. D. Arnett. 16 pp. and figs., March 16, 1962.

This report presents a theoretical treatment of the small-signal aspects of the generation of microwave power by passing an electron beam axially through a circular cylindrical cavity, where the beam interacts with the axial component of the electric field of the transverse magnetic modes of the cavity. The most favorable conditions for oscillation occur when the transit time is such that an unmodulated electron requires approximately $q + (1/4) \cos n\pi$ periods of the oscillation in traveling through the cavity. The

UNCLASSIFIED (over)

1. Radio frequency power – Generation
2. Electrons – Motion – Mathematical analysis
3. Cavity resonators
- I. Monotrons
- II. Arnett, H. D.

UNCLASSIFIED

small-signal electronic efficiencies are computed and plotted, and under the assumption that the power dissipated within the cavity can be attributed solely to skin-effect losses in the cavity walls, the unloaded starting currents are computed. It is shown that, from the standpoint of minimizing the starting current, the best mode to employ is the TM_{011} mode. Further, the starting current for the TM_{011} mode is minimized when the ratio of cavity length to cavity diameter is 1.544.

UNCLASSIFIED

UNCLASSIFIED

small-signal electronic efficiencies are computed and plotted, and under the assumption that the power dissipated within the cavity can be attributed solely to skin-effect losses in the cavity walls, the unloaded starting currents are computed. It is shown that, from the standpoint of minimizing the starting current, the best mode to employ is the TM_{011} mode. Further, the starting current for the TM_{011} mode is minimized when the ratio of cavity length to cavity diameter is 1.544.

UNCLASSIFIED

UNCLASSIFIED

small-signal electronic efficiencies are computed and plotted, and under the assumption that the power dissipated within the cavity can be attributed solely to skin-effect losses in the cavity walls, the unloaded starting currents are computed. It is shown that, from the standpoint of minimizing the starting current, the best mode to employ is the TM_{011} mode. Further, the starting current for the TM_{011} mode is minimized when the ratio of cavity length to cavity diameter is 1.544.

UNCLASSIFIED

UNCLASSIFIED

small-signal electronic efficiencies are computed and plotted, and under the assumption that the power dissipated within the cavity can be attributed solely to skin-effect losses in the cavity walls, the unloaded starting currents are computed. It is shown that, from the standpoint of minimizing the starting current, the best mode to employ is the TM_{011} mode. Further, the starting current for the TM_{011} mode is minimized when the ratio of cavity length to cavity diameter is 1.544.

UNCLASSIFIED